Novel biomaterial-based synovial fluid analysis reveals protective microRNA signatures in a mouse model of acute synovitis-driven osteoarthritis

Kei Takahata[1], Kohei Arakawa[2], Takashi Yasuda[3], Saaya Enomoto[4], Takuya Katashima[5], Takamasa Sakai[5], Takanori Kokubun[1, 6*]

1: Graduate School of Health, Medicine, and Welfare, Saitama Prefectural University, Saitama, Japan

2：Laboratory of Animal Regeneration Systemology, Department of Life Sciences, School of Agriculture, Meiji University, Kanagawa, Japan

3: Faculty of Advanced Life Sciences, Hokkaido University, Hokkaido, Japan

4: Saitama Prefecture General Rehabilitation Center, Saitama, Japan

5: Graduate School of Engineering, The University of Tokyo, Tokyo, Japan

6: Department of Physical Therapy, School of Health and Social Services, Saitama Prefectural University, Koshigaya, Saitama, Japan

[Author email addresses and ORCID]

Kei T; 2491006o@spu.ac.jp, 0000-0003-0649-5967

Kohei A; arakawa_k@meiji.ac.jp, 0000-0002-3454-2970

Takashi Y; t.yasuda@sci.hokudai.ac.jp, 0000-0002-7310-2492

Saaya E; 2481302r@spu.ac.jp, 0000-0002-4388-7938

Takuya K; katashima@g.ecc.u-tokyo.ac.jp, 0000-0001-6184-3835

Takamasa S; t-sakai@g.ecc.u-tokyo.ac.jp, 0000-0001-5052-0512

Takanori K; kokubun-takanori@spu.ac.jp, 0000-0001-6676-2356

[Full contact details of the corresponding author]

[1,6]Takanori Kokubun, Ph.D.

Graduate School of Health, Medicine, and Welfare, Saitama Prefectural University

820 San-nomiya, Koshigaya, Saitama, 343-8540, Japan

Tel: +81 48-973-417617

kokubun-takanori@spu.ac.jp

Running title: Protective signatures of synovial fluid miRNAs during acute synovitis-driven osteoarthritis in mouse model

Grants or other financial supporters of the study:

1 Japan Society for the Promotion of Science, Research Fellows (22J23384)

2 Grant-in-Aid for Japan Society for the Promotion of Science, Challenging Research (Exploratory)(21K19724)

All authors have no conflicts of interest related to the manuscript.

ABSTRACT

Objective: Synovial fluid micro-RNAs have been investigated to clarify the Osteoarthritis (OA) development, however, analyzing them in the murine models had not been established. The purpose of this study was to develop a novel biomaterial-based method to collect murine synovial fluid and elucidate onset mechanism of OA with acute synovitis and continuous mechanical stress.

Method: Twelve-week-old C57BL/6J males (n = 72) were divided to the ACL-Transection (ACL-T), ACL-rupture (ACL-R), and Intact groups. We performed joint instability test and histological analysis for cartilage degeneration and synovitis at 2, 6, and 10 weeks. Real time PCR was conducted for articular cartilage at 2 weeks and synovium at 2, 6, and 10 weeks. Tetra-slime was injected into the knee joint and solidified slime including synovial fluid was analyzed in digital PCR at 2 weeks.

Results: Although no difference was observed in joint instability between both ACL injury models, acute synovitis and cartilage degeneration were induced in the ACL-T group at 2 weeks. The ACL-T group also increased Mmp-3, Tnf-α, Ifn-γ, and inos in synovium, and miR145-5p and miR149-5p in synovial fluid compared to the ACL-R group. However, no histological and biological differences were observed at 6 and 10 weeks.

Conclusion: Acute synovitis caused secondary cartilage degeneration through MMP-3, TNF-α, and M1 macrophage activation in the synovium during the early stage,

whereas synovial fluid miR145-5p and miR149-5p were produced to prevent the progression. However, mechanical stress had a much greater impact on cartilage degeneration in the long run rather than synovitis.

Key Words:

Osteoarthritis, Synovial fluid, Synovitis, Mechanical stress, miRNA, biomaterials

99 # Introduction

100 Knee Osteoarthritis (OA) is one of the most common musculoskeletal diseases,
101 characterized by whole-joint pathology, including synovitis and subchondral bone sclerosis,
102 resulting from cartilage degeneration[1]. These structural changes affect each other via synovial
103 fluid and progress irreversibly, as articular cartilage is avascular and has a poor healing
104 capacity. To achieve the prevention of cartilage degeneration, elucidating the intra-articular
105 changes that occur during early OA progression before cartilage degeneration is required;
106 however, it is assumed that early detection is difficult in humans due to the variability of
107 symptoms and disease progression in the early stages of cartilage degeneration. [2, 3]

108 In the knee joint space, synovial fluid fills and mediates bidirectional interaction
109 between the joint tissues. Synovial fluid is an ultrafiltrate of blood plasma and is primarily
110 composed of hyaluronan and lubricin, which play a significant role as a joint space lubricant
111 and a nutrient source for intra-articular tissues. [4] Previous studies have reported that
112 Interleukin (IL)-6, IL-8, and Tumor Necrosis Factor (TNF)-α in synovial fluid are correlated
113 with OA severity. [5] Additionally, Matrix Metalloproteinase (MMP)-3 could be a biomarker
114 for detecting early-stage OA. [6] Furthermore, circulating microRNAs (miRNAs) in the
115 synovial fluid have been recently highlighted as a novel biomarker. [7] miRNAs are short, non-
116 coding RNAs that are typically 18-25 nucleotides in length, which are used to investigate
117 various diseases as they are stable compared to other RNAs degraded by ribonucleases.[8] It has

118 been reported that miR-23a-3p, miR-24-3p, miR-27b-3p, miR-29c-3p, miR-34a-5p, and miR-
119 186-5p in the synovial fluid were expressed in the late-stage OA compared to the early-stage.
120 [9] In addition, synovial fluid miR-210 increased significantly in the early and late-stage OA
121 than in healthy individuals. [10] Therefore, synovial fluid has been identified as a potential
122 target to detect the intra-articular environment in the OA progression. Many clinical studies
123 have been investigating the synovial fluid biomarker to find OA earlier in human [11], which
124 has yet to be established. Thus, preclinical experiments using animal models are crucial for
125 understanding the mechanism of OA onset. However, synovial fluid analysis, especially for
126 miRNAs in rodent models, is limited because the amount of synovial fluid is tiny. In a few
127 studies, joint lavage was performed as follows: 25-50 μL of saline was initially injected into
128 the knee joint, and then the synovial fluid was drawn out.[12-14] However, it is difficult to
129 collect a sufficient amount of synovial fluid and present relevant data due to the tiny knee
130 joints in mice.[15]

131 Recently, many kinds of biomaterials were developed and applied for drug delivery,
132 tissue engineering, and medical diagnostics. [16-18] Tetra-slime is composed of reversible
133 boronic ester bonds between phenylboronic acid and diol groups, and its stiffness can be
134 changed by adjusting the precursor concentration and pH. Moreover, it can also be dissolved
135 by sorbitol as sugars attach to phenylboronic acid and cleave ester bonds. [19] Based on these
136 material properties, we hypothesized that harvesting and dissolving the solidified Tetra-Slime,

137 which was injected into the knee joint, would allow for the efficient collection of synovial
138 fluid. The purpose of this study was to develop a novel method to analyze synovial fluid
139 miRNAs in murine knee joints using biomaterials, Tetra-slime,[20] instead of joint lavage
140 methods to reveal the onset mechanism of knee OA based on the synovial fluid dynamics.
141 Using this method in surgical Anterior Cruciate Ligament Transection (ACL-T) and Non-
142 Invasive ACL rupture (ACL-R) mice models, we aimed to elucidate the characteristics of
143 each rodent model in terms of acute inflammation and continuous mechanical stress, which
144 serves fundamental insights to understand human pathology in detail.
145

146 # MATERIALS AND METHODS

147 **Animals and Experimental Design**

148 This study was approved by the Animal Research Committee of Saitama Prefectural
149 University (approval number: 2020-6). The animals were handled according to relevant
150 legislation and institutional guidelines for humane animal treatment. Seventy-two 12-week-
151 old C57BL/6 male mice were randomized into the Invasive ACL-T group (n = 36) and Non-
152 Invasive ACL-R group (n = 36). The contralateral knee joint in the ACL-R group was used as
153 the control group. Six mice in each group were sacrificed at 2, 6, and 10 weeks, and the target
154 tissues were collected for each analysis (Fig. 1). All mice were housed in plastic cages under a

155 12-hour light/dark cycle. The mice were allowed unrestricted movement within the cage and

156 had free access to food and water.

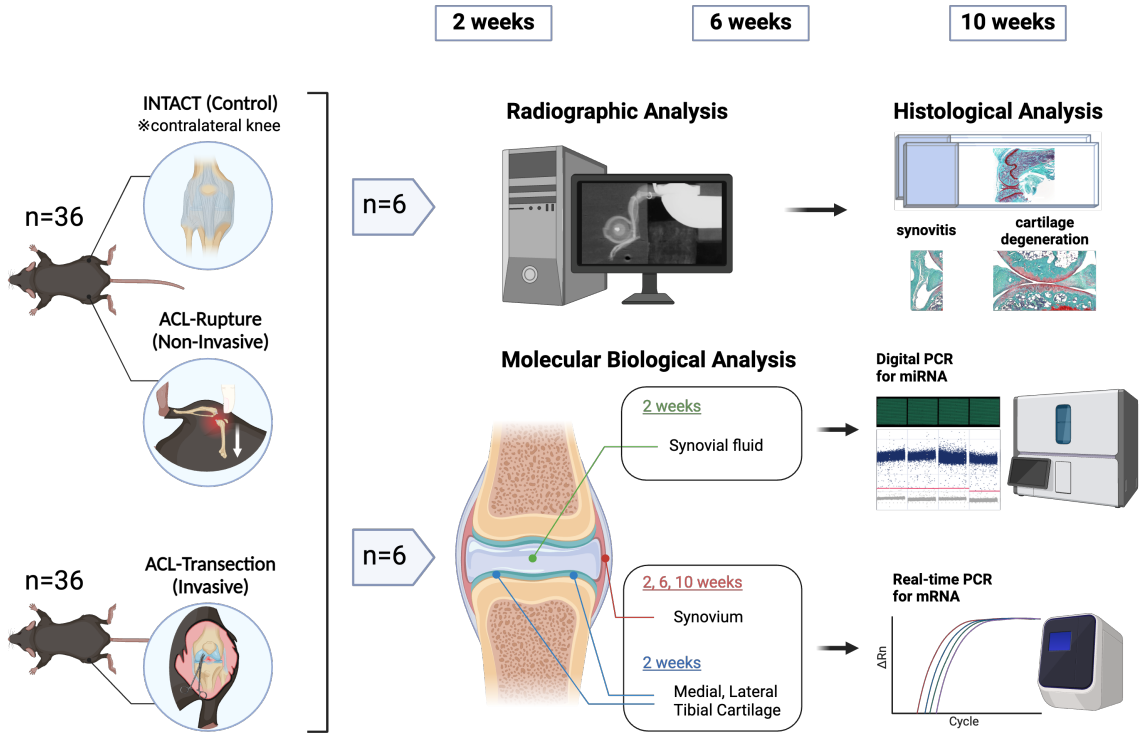

157

158 Fig. 1. Experimental design. We made the Invasive ACL-T, Non-Invasive ACL-R, and

159 Control groups. Contralateral knee in the ACL-R model was used as Control group. At 2, 6,

160 and 10 weeks, anterior drawer test and histological analysis for synovitis and cartilage

161 denegation in the medial and lateral compartments were performed. Articular cartilage at 2

162 weeks and synovium at 2, 6, and 10 weeks were harvested, and mRNAs were analyzed in real

163 time PCR. In addition, synovial fluid was collected at 2 weeks and miRNAs level were

164 assessed.

165

166

167 **Creating ACL-T and ACL-R models**

168 All procedures were performed on the left knee joint of each mouse under a
169 combination of anesthetics (medetomidine, 0.375 mg/kg; midazolam, 2.0 mg/kg; and
170 butorphanol, 2.5 mg/kg). The medial joint capsule was cut to expose the intra-articular joint.
171 ACL was transected with scissors to avoid causing injuries to other tissues. After checking the
172 anterior tibial translation manually, the joint capsule and skin incision were closed with 5-0
173 nylon threads. The ACL-R model was created based on our previous study.[21] Briefly, the knee
174 joint was fixed at 90 degrees using surgical tape on a stand, then the force along the long axis
175 of the femur was applied by the thumb's tip slowly and carefully. Applied force was stopped
176 quickly after hearing a distinct popping sound, which indicates ACL rupture; thereafter,
177 anterior tibial translation was confirmed manually as well.
178
179 **Ex vivo radiographic analysis for knee joint instability**
180 After dissection at each time point, knee joints were collected (each group, n = 6) and
181 an anterior drawer test was performed to evaluate joint instability (Fig. 2A). Based on our
182 previous study [21, 22], the proximal tibia was pulled forward with a constant force spring (0.05
183 kgf; Sanko Spring Co., Ltd., Fukuoka, JPN), and X-ray images were taken at this position. In
184 the acquired image, the tibial tuberosity and the anterior end of the femoral condyle were set
185 as landmarks, then the anterior tibial displacement was measured by the linear distance from

186 the perpendicular line from the anterior end of the femoral condyle to the tibial tuberosity

187 using Image J (National Institutes of Health, Bethesda, MD, USA).

188

189 **Histological analysis for cartilage degeneration and synovitis**

190 Knee joints were fixed using 4% paraformaldehyde for 1 day, decalcified in 10%

191 ethylenediaminetetraacetic acid for 2 weeks, dehydrated in 70% and 100% ethanol and

192 xylene, and embedded in paraffin blocks after performing radiographic analysis. The samples

193 were cut in the sagittal plane (thickness, 7 μm) using a microtome (ROM-360; Yamato Kohki

194 Industrial Co., Ltd., Saitama, JPN). Then, safranin-O/fast green staining was performed to

195 assess the articular cartilage degeneration with the Osteoarthritis Research Society

196 International (OARSI) histopathological grading system [23] and synovitis score [24] in the medial

197 and lateral compartments. These scores were assessed by two independent observers blinded

198 to all other sample information. We evaluated the contact area not covered by the meniscus on

199 the tibial plateau and the synovium located inside the infrapatellar pad. The mean of the

200 observer's scores was used as a representative value.

201

202 **Real-time PCR for articular cartilage and synovium**

203 Articular cartilage on the medial and lateral tibial plateau at 2 weeks and synovium at

204 2, 6, and 10 weeks were collected and stored in a deep freezer until analysis (each group, n =

205 6). Based on the manufacturer's instructions, total RNA was extracted from these tissues

206 using the ISOGEN (NIPPON GENE CO., LTD., Tokyo, JPN). cDNA synthesis was

207 performed from the total RNA by Thermal Cycler Palm-Cycler (Corbett Research, SYD,

208 AUS) with High-Capacity cDNA Reverse Transcription kit (Applied Biosystems, CA, USA).

209 Subsequently, real-time PCR was conducted to assess the expression of following genes using

210 the StepOne-Plus system (Applied Biosystems, Waltham, MA, USA); *Mmp-*

211 *3*(Mm00440295), Tissue inhibitor of metalloproteinase-1 (*Timp-1:* Mm01341361),

212 Transforming growth factor-β1 (*Tgf-β1:* Mm01178820), *Tnf-α* (Mm00443258), *Il-1β*

213 *(*Mm00434228), *Il-6* (Mm00446190), *Il-10* (Mm01288386), Interferon-γ (*Ifn-*

214 *γ* :Mm01168134), inducible nitric oxide synthase（*inos* :Mm00440502_m1), and Toll like

215 receptor-4 (*Tlr4* :Mm00445273_m1). We used Glyceraldehyde-3-phosphate dehydrogenase

216 (*Gapdh* :Mm99999915) as a housekeeping gene, and relative expression of genes was

217 detected by the 2-△△Ct method. [25]

218

219 **Digital PCR for synovial fluid miRNA using Tetra-Slime**

220 In this study, we selected the Tetra-slime to collect the murine synovial fluid. 4-arm

221 PEG BFA and 4-arm PEG Gluconic (XIAMEN SINOPEG BIOTECH CO., LTD., Fujian,

222 CHN) were resolved with 50 mM phosphate-buffered saline (pH 3.0) to adjust 0.2 g/ml

223 concentration respectively. We injected both solutions by 25 μL into the knee joint for live

224 mice, then kept the needle for a while to avoid leaking the solution (Fig. 7A). After 3 minutes,
225 mice were sacrificed and the quadriceps and patellar were removed to expose the intra-
226 articular joints, then solidified Tetra-Slime was collected. We added 100 μL of sorbitol
227 solution with a 0.5 g/ml concentration to the collected Tetra-Slime and stirred slowly to
228 dissolve and separate from the surrounding intra-articular tissue, then obtained the pure
229 solution with synovial fluid biomolecules released. Based on the manufacturer's instructions,
230 miRNA was extracted from the synovial fluid solution using the miRNeasy Micro Kit
231 (QIAGEN, LTD. Tokyo, JPN). cDNA synthesis was performed by QIAamplifier 96
232 (QIAGEN, LTD. Tokyo, JPN) with miRCURY LNA RT Kit (QIAGEN, LTD. Tokyo, JPN).
233 Subsequently, digital PCR (dPCR) was conducted using the QIAcuity One (QIAGEN, LTD.
234 Tokyo, JPN) and target genes were *hsa-miR-145-5p* (YP00204483) and *hsa-miR-149-5p*
235 (YP00204321). We normalized the target gene with the housekeeping gene, 5S rRNA
236 (YP00203906), for each sample, and then calculated the relative expression level by
237 standardizing with the Control group. UniSp6 (YP00203954) was also used as a spike-in
238 control.
239

240 **Statistical analysis**

241 Statistical analysis was performed using RStudio version 1.4.1106. For the results of
242 anterior tibial displacement by the anterior drawer test, relative expression of genes in

243 synovium and cartilage by real-time PCR, and miRNA data measured using dPCR, one-way
244 analysis was performed initially, then the Tukey-Kramer test was used as a post-hoc test. We
245 utilized the value of ΔCt for the real-time PCR data and the relative expression value for the
246 dPCR data. Whereas the Kruskal-Wallis test was used to compare the OARSI and synovitis
247 scores, and the Steel-Dwass method was used for the subsequent multiple comparisons.
248 Parametric data are expressed as the means ± 95% confidence intervals (CI); in contrast, the
249 non-parametric data are expressed as the medians ± interquartile ranges. Statistical
250 significance was set at $p < 0.05$. CIs were shown in the Supplementary data.
251

252 Results

253 **ACL-T and ACL-R groups showed similar joint instability**

254 The anterior displacement in the ACL-T and ACL-R groups was significantly higher
255 than that in the Control groups at 2 weeks (ACL-T vs. Control, $p < 0.001$, ACL-R vs. Control,
256 $p < 0.001$), 6 weeks (ACL-T vs. Control, $p < 0.001$, ACL-R vs. Control, $p < 0.001$), and 10
257 weeks (ACL-T vs. Control, $p < 0.001$, ACL-R vs. Control, $p < 0.001$). However, there was no
258 significant difference between the ACL-T and ACL-R groups at all time points. These results
259 suggested that the effect of mechanical stress on OA progression was identical in both ACL-
260 deficient models.
261

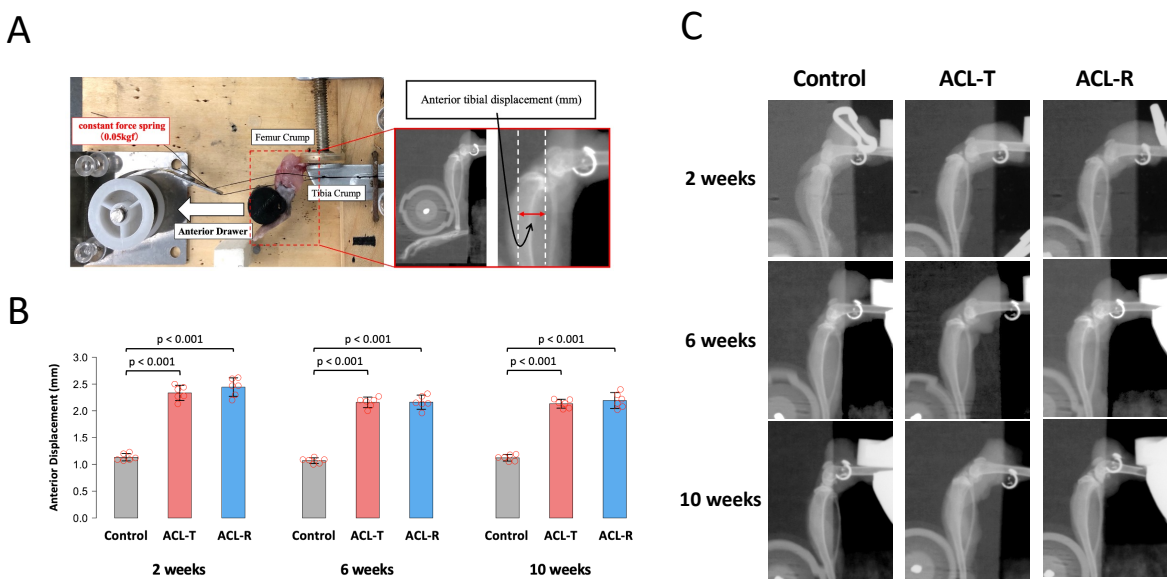

Fig. 2. Evaluation of the joint instability *ex vivo* using soft X-ray and original anterior drawer device. At 2, 6, and 10 weeks, the amount of anterior tibial displacement was significantly increased in the ACL-T and ACL-R groups compared to that in the Control group. However, there was no significant difference between both ACL injury models. Data are presented as the mean ± 95% CI.

ACL-T group induced acute synovitis in the early stage

For the medial compartment, severe synovitis with increased cellularity, enlargement of the synovial lining cell layer, and inflammatory infiltration was observed in the ACL-T group (Fig. 3A). Moderate synovitis with cell multiplication and cell layer enlargement was confirmed in the ACL-R group. Compared with the Control group, synovitis score was significantly higher in the ACL-T group ($p = 0.009$) and ACL-R group ($p = 0.012$) (Fig 3B). Interestingly, ACL-T group increased score significantly compared with the ACL-R group (p

276 = 0.032). At 6 weeks, moderate synovitis characterized by some enlargement and increased
277 cellularity developed in both ACL-deficient groups, and the synovitis score in the ACL-T
278 group ($p = 0.01$) and ACL-R group ($p = 0.01$) was significantly higher than in the Control
279 group. At 10 weeks, similar moderate to severe synovitis was observed in both ACL-deficient
280 groups, and the synovitis score in the ACL-T group ($p = 0.009$) and ACL-R group ($p = 0.01$)
281 was significantly elevated compared to the Control group.

282 For the lateral compartment, moderate and mild synovitis occurred in both ACL-
283 deficient groups. Synovitis score was significantly higher in the ACL-T group ($p = 0.009$) and
284 ACL-R group ($p = 0.01$) compared with the Control group (Fig. 3C-D). At 6 and 10 weeks,
285 moderate synovitis was observed in the ACL-T and ACL-R groups, and both synovitis scores
286 increased significantly compared with the Control group (6 weeks: ACL-T vs. Control, $p =$
287 0.01; ACL-R vs. Control, $p = 0.013$, 10 weeks: ACL-T vs. Control, $p = 0.016$; ACL-R vs.
288 Control, $p = 0.01$).

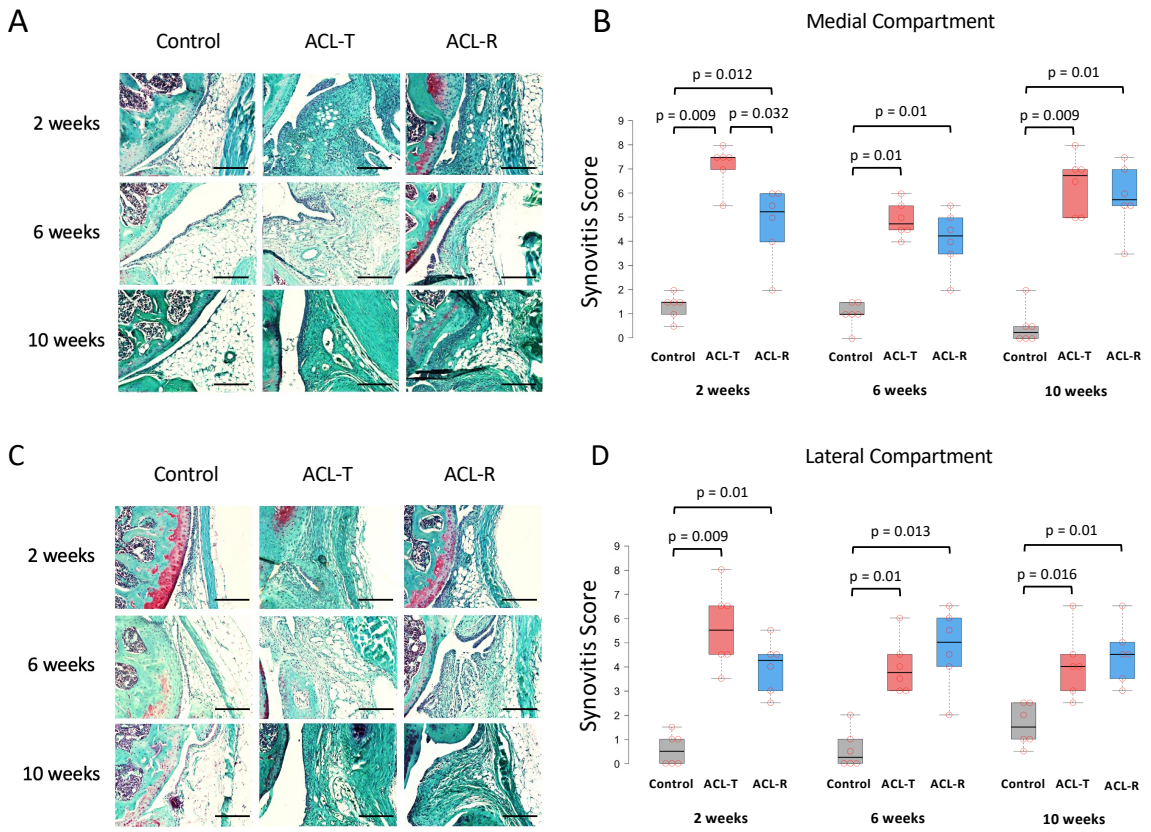

Fig. 3. Histological analysis of synovitis using safranin-O/fast green staining and synovitis score. (A-B) In the medial compartment, the synovitis score in the ACL-T and ACL-R groups was significantly higher than that in the Control group at 2 weeks. Moreover, the score in the ACL-T group was also elevated significantly compared to the ACL-R group. At 6 and 10 weeks, both ACL injury groups significantly increased the synovitis score compared with the Control group. (C-D) In the lateral compartment, the ACL-T and ACL-R groups exhibited a significant increase of synovitis score compared to the Control group at all timepoints. Data are presented as the median ± interquartile range. Black scale bar, 100 μm.

Secondary cartilage degeneration was induced by acute synovitis in the ACL-T group

300 To examine the tissue interaction between early synovitis and cartilage degeneration,
301 histological analysis was performed. For the medial compartment, some fibrillation of the
302 superficial cartilage was observed in the ACL-T and ACL-R groups at 2 weeks (Fig. 4A).
303 Additionally, small clefts and loss of cartilage were confirmed only in the ACL-T group. The
304 OARSI score of the ACL-T group was significantly higher than that of the Control group ($p =$
305 0.009) (Fig. 4B). At 6 weeks, cartilage fibrillation and mild to moderate vertical cracks into
306 the calcified layer developed in both ACL-deficient groups. Compared with the Control
307 group, the OARSI score was significantly elevated in the ACL-T group ($p = 0.022$) and ACL-
308 R group ($p = 0.014$). At 10 weeks, moderate to severe cartilage degeneration with loss of the
309 superficial layer was observed in both ACL-deficient groups. Compared with the Control
310 group, the OARSI score significantly increased in the ACL-T group ($p = 0.01$) and ACL-R
311 group ($p = 0.01$).
312 For the lateral compartment, cartilage degeneration with loss of safranin staining,
313 small fibrillation, and vertical clefts was confirmed in the only ACL-T group at 2 weeks (Fig.
314 4C). The OARSI score in the ACL-T group was significantly higher compared with that in
315 the Control group ($p = 0.018$) and ACL-R group ($p = 0.02$) (Fig. 4D). At 6 weeks, small
316 fibrillation and clefts in the superficial cartilage layer occurred in both ACL-deficient groups;
317 however, there was no significant difference in the OARSI score between all groups. At 10
318 weeks, mild cartilage degeneration with small fibrillation and vertical clefts in the superficial

319 cartilage layer was observed in both ACL-deficient groups. Compared with the Control

320 group, the OARSI score was significantly higher in the ACL-T group (p = 0.012) and ACL-R

321 group (p = 0.044). In summary of the histological analysis, the ACL-T group induced acute

322 synovitis and cartilage degeneration in the first 2 weeks compared with the ACL-R group,

323 although no difference in the joint instability. Cartilage degeneration in both ACL-deficient

324 models progressed in the late stage, as well as synovitis.

325

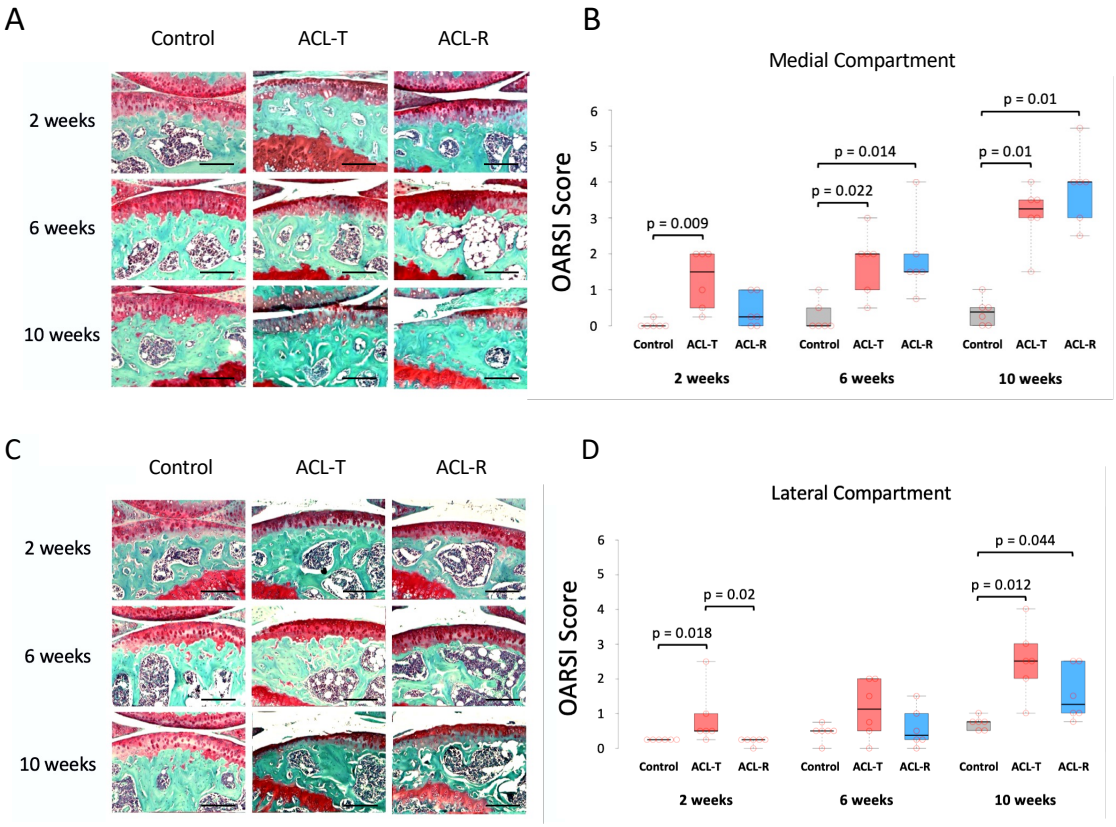

326

327 Fig. 4. Histological analysis of cartilage degeneration using safranin-O/fast green staining and

328 OARSI score. (A-B) In the medial compartment, the OARSI score in the ACL-T group was

329 significantly higher than that in the Control group at 2 weeks. At 6 and 10 weeks, both ACL

330 injury groups significantly increased the OARSI score compared with the Control group. (C-
331 D) In the lateral compartment, the OARSI score in the ACL-T group increased significantly
332 compared the Control and ACL-R groups at 2 weeks. At 10 weeks, both ACL injury groups
333 exhibited a significant increase of OARSI score compared to the Control group. Data are
334 presented as the median ± interquartile range. Black scale bar, 100 μm.
335

336 **ACL-R group induced catabolic factors and inflammation cytokine expression in the**
337 **articular cartilage**

338 To explore the molecular mechanism between acute synovitis and cartilage
339 degeneration, we performed real-time PCR for the articular cartilage at 2 weeks because
340 cartilage degeneration occurred in the whole area moderately after 6 weeks. In the medial
341 tibial cartilage compared with the Control group, ACL-T group significantly increased the
342 expression of *Mmp-3* ($p < 0.001$), *Timp-1* ($p = 0.009$), and *Tnf-α* ($p = 0.008$) (Fig. 5A-C).
343 ACL-R group also significantly exhibited an increase of *Mmp-3* ($p < 0.001$), *Timp-1* ($p <$
344 0.001), and *Tnf-α* ($p < 0.001$) compared with the Control group. Moreover, *Tnf-α* in the ACL-
345 R group was significantly higher than in the ACL-T group ($p = 0.005$) (Fig. 5C).

346 In the lateral tibial cartilage, ACL-T group significantly exhibited an increase of
347 *Mmp-3* ($p < 0.001$) and *Timp-1* ($p = 0.036$) compared with the Control group (Fig. 5E-F).
348 *Mmp-3*, *Timp-1*, and *Tnf-α* in the ACL-R group were significantly upregulated compared with

349 the Control group (*Mmp-3*; p < 0.001, *Timp-1*; p < 0.001, *Tnf-α*; p = 0.008) and ACL-T group

350 (*Mmp-3*; p = 0.03, *Timp-1*; p = 0.036, *Tnf-α*; p < 0.001) (Fig. 5E-G). However, no significant

351 differences were observed in the *Ifn-γ* between all groups for the medial and lateral tibial

352 cartilage (Fig. 5D, H). *Tgf-β1*, *Il-1β*, *Il-6*, and *Il-10* were exhibited in the Supplementary

353 Figure 1.

354

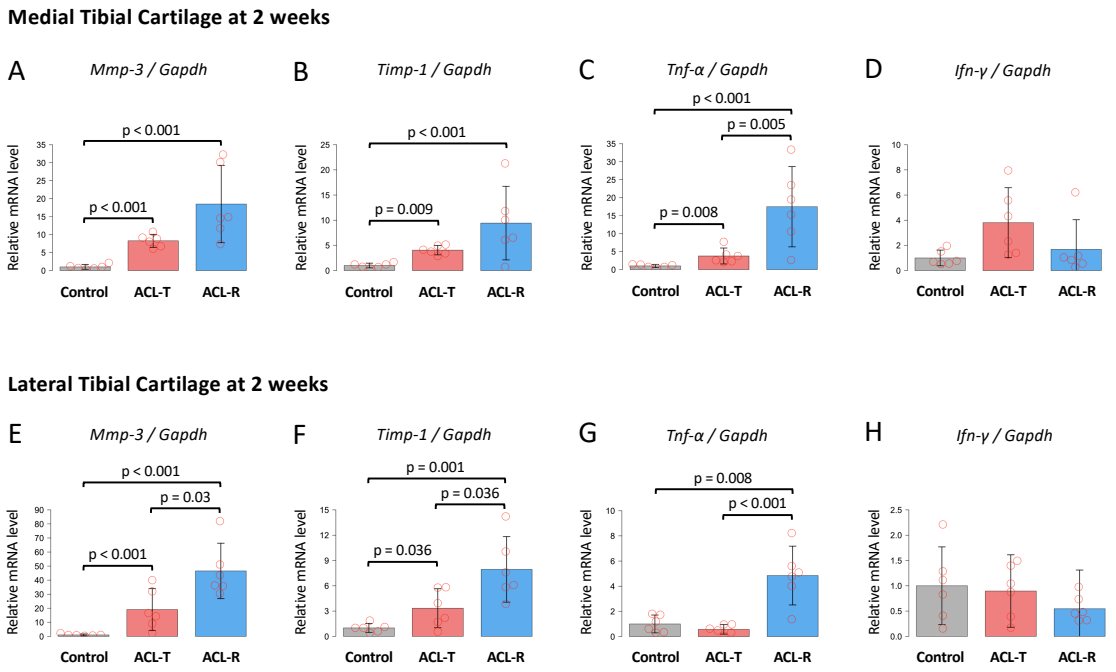

355

356 Fig. 5. Real time PCR analysis for medial and lateral tibial articular cartilage at 2 weeks. (A-

357 D) In the medial cartilage, *Mmp-3*, *Timp-1*, and *Tnf-α* expression in the ACL-T and ACL-R

358 groups were significantly increased compared to that in the Control group. In addition, the

359 ACL-R group exhibited a significant increase of *TNF-α* compared to the ACL-T group. (E-H)

360 In the lateral cartilage, the expression of *Mmp-3*, *Timp-1*, and *Tnf-α* in both ACL injury

361 groups were significantly upregulated compared to that in the Control group. *Mmp-3* and

362 *Timp-1* were also significantly increased in the ACL-R group compared to the ACL-T group.

363 Data are presented as the mean ± 95% CI.

364

365 **ACL-T group increased the expression of catabolic factors, inflammatory cytokines, and**

366 **M1 macrophage markers in the synovium**

367 At 2 weeks, *Mmp-3* expression was significantly higher in the ACL-T group ($p <$

368 0.001) and ACL-R group ($p < 0.001$) than the Control group (Fig. 6A). Furthermore, the

369 ACL-T group also exhibited an increase of *Mmp-3* expression significantly compared with

370 the ACL-R group ($p = 0.048$). *Timp-1* was elevated significantly in the ACL-T ($p = 0.002$)

371 and ACL-R group ($p < 0.001$) compared with the Control group (Fig. 6B). The ACL-T group

372 significantly increased *Tnf-α*, *Ifn-γ*, and *inos* compared with the Control (*Tnf-α*; $p = 0.001$, *Ifn-*

373 *γ*; $p = 0.021$, *inos*; $p = 0.017$) and ACL-R group (*Tnf-α*; $p = 0.004$, *Ifn-γ*; $p = 0.012$, *inos*; $p =$

374 0.009) (Fig. 6C-E). However, no significant difference was observed in the *Tlr4* expression

375 among groups (Fig. 6F). The results for *Tgf-β1*, *Il-1β*, *Il-6,* and *Il-10* at 2 weeks, all results at

376 6 weeks, and 10 weeks were described in the Supplementary Figures 2-4.

377 In summary, the RT-qPCR results showed the increased expression of the *Mmp-3*,

378 *Timp-1* of *Mmp-3* inhibitor [26], and *Tnf-α* in cartilage of the ACL-R group, although it induced

379 less synovitis and cartilage degeneration. Unlike the results of cartilage, synovium in the

380 ACL-T group showed upregulation of *Ifn-γ,* M1 macrophage polarization factor, and *iNos*,

381 M1 macrophage marker[27-30] , in addition to *Mmp-3* and *Tnf-α*. However, the *Mmp-3* and *Tnf-α*

382 expressions were not increased at 6 and 10 weeks.

383

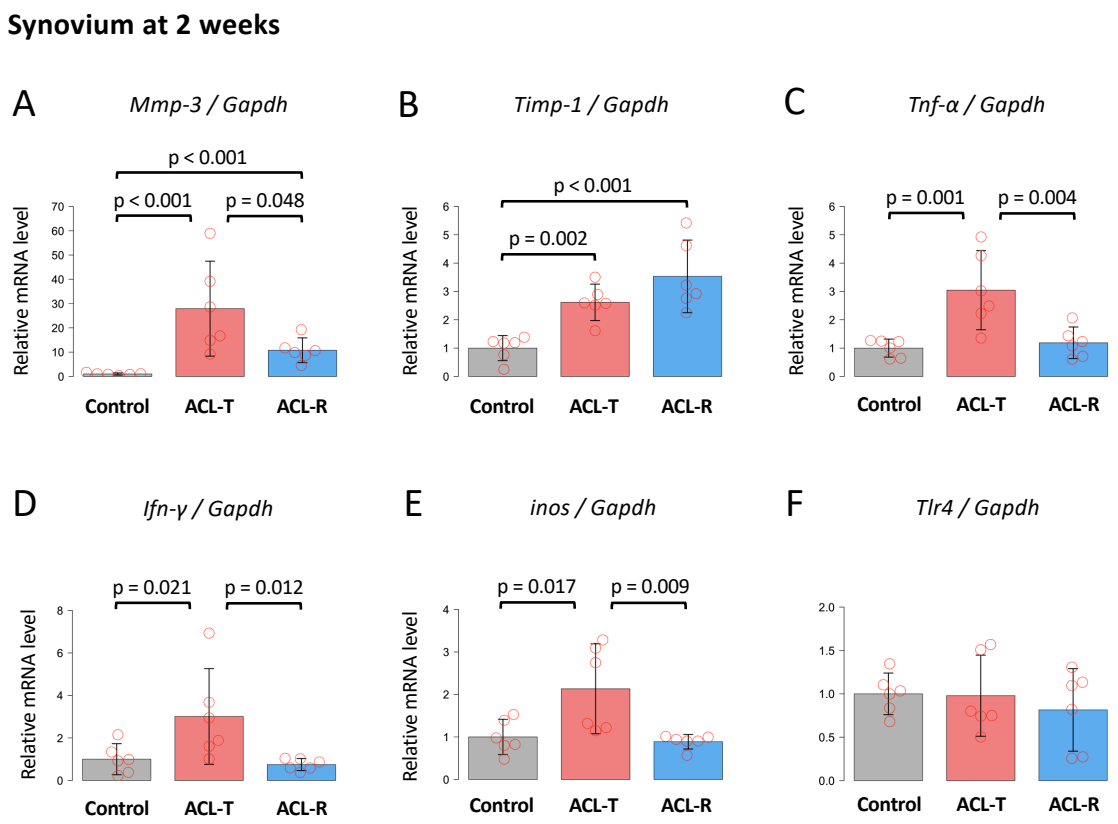

384

385 Fig. 6. (A) Real time PCR analysis for synovium at 2 weeks. (A) *Mmp-3* expression in the

386 ACL-T and ACL-R groups were significantly higher than that in the Control group.

387 Moreover, the ACL-T group also significantly increased it compared to the ACL-T group. (B)

388 *Timp-1* in both ACL injury groups was upregulated compared to that in the Control group.

389 (C-E) The ACL-T group exhibited a significant increase of *Tnf-α, Ifn-γ, and inos* compared to

390 the Control and ACL-R group. (F) No difference was observed in the *Tlr4* expression level

391 between groups. Data are presented as the mean ± 95% CI.

392

393 **The expression of miR145-5p and miR149-5p in the synovial fluid increased in the ACL-**

394 **T group**

395 To verify the effect of using biomaterial for dPCR, we initially analyzed 5S rRNA

396 expression in only Tetra-Slime as a negative control. Compared with the Tetra-slime

397 including synovial fluid, concentration of 5s rRNA in only Tetra-Slime group was obviously

398 lower although Unisp6 of spike-in control was observed (Supplementary Figure 5). The

399 expression of miR145-5p[31] and miR149-5p[32, 33], which are downregulated by TNF-α, was

400 investigated. dPCR results showed the increased expression of *miR145-5p* and *miR149-5p* in

401 the ACL-T group compared with other groups, although this difference was not statistically

402 significant (Fig. 7B, C).

403

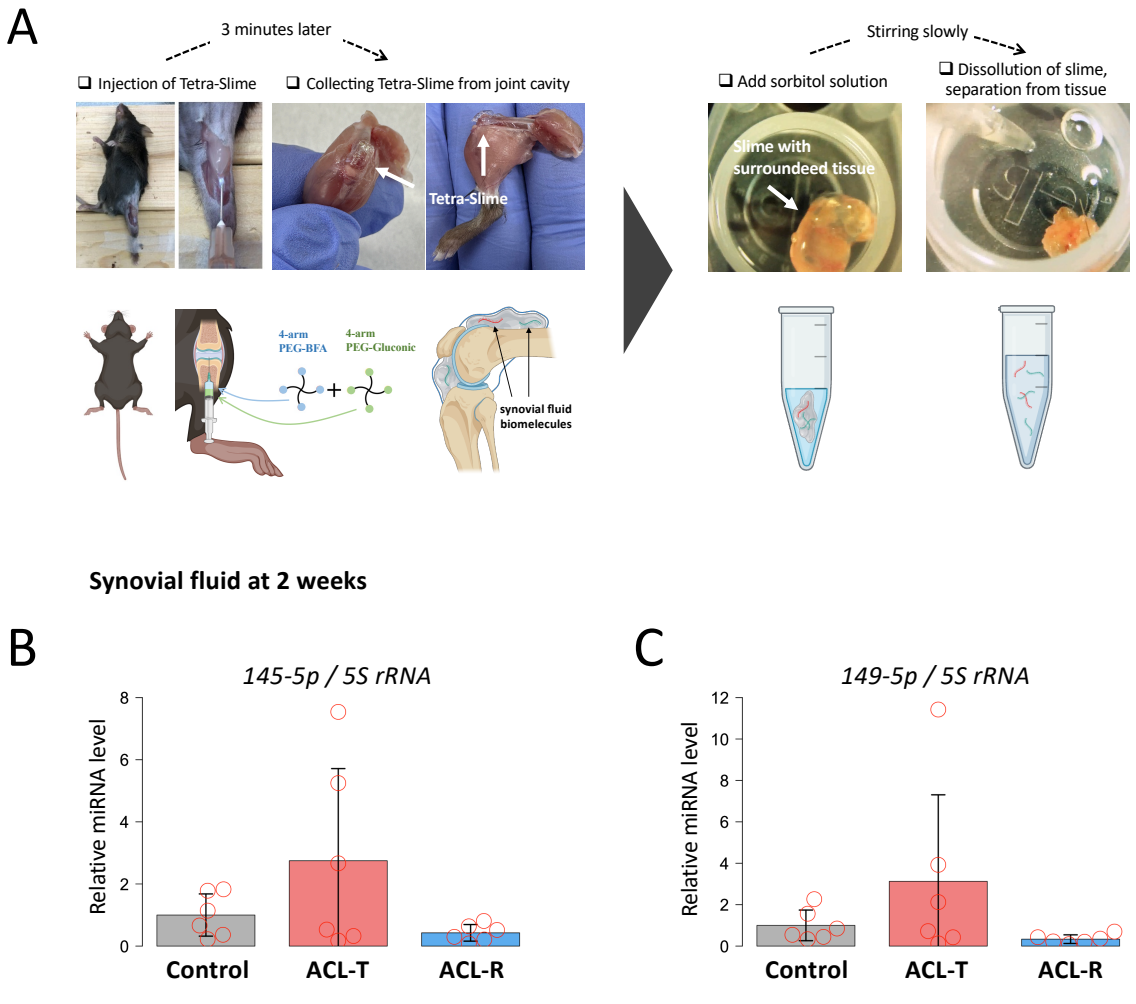

Fig. 7. (A) Conceptual diagram of a novel method to collect synovial fluid biomolecules in the murine knee joints using Tetra-Slime. After dissolving 4-arm PEG-BFA and 4-arm PEG-Gluconic in 50 mM phosphate-buffered saline (pH 3.0) and adjusting the concentration to 0.2 g/ml, 50 µl was injected into the knee joint. 3 minutes later, solidified Tetra-Slime including synovial fluid was collected and it was resolved by 100 µL of sorbitol solution with a 0.5 g/ml concentration to separate from the surrounding intra-articular tissue. (B-C) The ACL-T group exhibited an increase of miR145-5p and miR149-5p expression in synovial fluid compared to the Control and ACL-R groups at 2 weeks. Data are presented as the mean ± 95% CI.

413 # Discussion

414 Synovial fluid analysis contributes to understanding molecular changes within knee
415 joint capsule and detecting OA earlier. However, analysis methods for mice had not been
416 established. In this study, we developed a novel method to collect and analyze synovial fluid
417 miRNAs in murine knee joints using Tetra-slime, which can adjust its stiffness. Using this
418 method, we aimed to investigate knee OA pathology in each Invasive and Non-Invasive ACL
419 injury mouse models in terms of tissue-interaction via synovial fluid. Our data clarified that
420 acute synovitis in the ACL-T model induced secondary cartilage degeneration in the early
421 stage compared with the ACL-R model; however, the progression of these histological
422 changes was identical between both models in the late stage. Real-time PCR revealed that
423 *Mmp-3*, *Tnf-α*, and M1 macrophage activation in synovium might be involved in the
424 secondary cartilage degeneration. We successfully established a novel method for analyzing
425 murine synovial fluid, and dPCR revealed that circulating *miR145-5p* and *miR149-5p* in
426 synovial fluid may suppress OA progression caused by acute synovitis.

427 Mechanical stress plays a significant role in maintaining intra-articular homeostasis;
428 however, excessive stress induces synovitis and cartilage degeneration. During the early stage
429 of OA progression, synovitis is generally initiated and driven by damage-associated
430 molecular patterns (DAMPs) released from the extracellular matrix to the synovial fluid.[34-37]
431 DAMPs activate TLRs in the synovium, leading to cartilage degeneration through the

432 inflammatory mediators and MMPs.[38, 39] In this study, we demonstrated that the ACL-T
433 group significantly induced synovitis at 2 weeks compared with the ACL-R group. However,
434 there was no difference in joint instability between groups. Furthermore, real-time PCR
435 revealed no differences in *Tlr4* expression, the receptor for DAMPs [39] in the synovium,
436 among all groups. Considering that synovitis is generally induced by DAMPs through
437 cartilage degeneration, our result indicates that acute synovitis at 2 weeks in the ACL-T group
438 is attributed to the surgical intervention, not secondary pathogenesis. Previous studies
439 reported that cartilage degeneration following ACL injury initiates in the medial compartment
440 due to joint instability. [40-42] However, the OARSI score in the lateral compartment of the
441 ACL-T group was significantly higher than that of the ACL-R group at 2 weeks, suggesting
442 that acute synovitis might cause secondary cartilage degeneration in the early stage.
443 We revealed the effect of acute synovitis on cartilage degeneration during the OA
444 progression, then performed molecular biological analysis to examine the tissue interaction
445 between synovium and cartilage. MMP-3 in the synovium of OA patients was positively
446 related to the severity [43], and it degrades cartilage ECM and activates other serine proteases
447 besides MMP-1, MMP-9, and MMP-13. [44] Previous studies have shown that the depletion of
448 synovial macrophages suppresses MMP-3 expression both in vivo [45] and in vitro. [46] Our data
449 showed that *Mmp-3*, *Tnf-α*, *Ifn-γ*, and *inos* were upregulated in the synovium of the ACL-T
450 group at 2 weeks, which supported a previous study. This suggests that M1 macrophages

451 likely affected the tissue interaction between acute synovitis and secondary cartilage

452 degeneration. Unlike the synovial molecular changes, the expression of *Mmp-3* and *Tnf-α* in

453 the cartilage increased significantly in the ACL-R group compared with the ACL-T group at

454 the same time point. These results suggest that articular cartilage may initiate intra-articular

455 degeneration more preferentially than synovium in the OA induced by joint instability and

456 less inflammation, which supports our previous study. [21] The expression of *Timp-1*, which is

457 an MMP-3 inhibitor [26], was also elevated significantly; therefore, it is estimated that cartilage

458 degeneration occurred slightly in the ACL-R model at 2 weeks.

459 Synovial fluid is the most suitable biofluid for exploring the onset mechanism of OA

460 because it directly reflects the changes in various intra-articular tissues. The importance of

461 miRNA epigenetic regulation as a cellular communication is becoming increasingly

462 recognized, and many studies have recently demonstrated its effectiveness in the synovial

463 fluid of OA patients. [47, 48] However, no study investigated the changes in synovial fluid

464 miRNA in the mice OA model due to the difficulty of collection and analysis. Here, we

465 established a novel method to collect synovial fluid effectively from the murine knee joint

466 using Tetra-Slime. dPCR showed a non-specific reaction of Tetra-Slime to 5s rRNA

467 expression (Supplementary result), meaning that it enabled the analysis of synovial fluid

468 components accurately. Previous studies reported that TNF-α downregulated both miR145-5p

469 [31] and miR149-5p [32] in chondrocytes, leading to cartilage degeneration. However, our results

470 clarified that circulating *miR145-5p* and *miR149-5p* expression in synovial fluid increased
471 moderately at 2 weeks in the ACL-T group despite inducing moderate OA pathology. This
472 suggests that miR145-5p and miR149-5p in synovial fluid might be produced from
473 chondrocytes to protect against secondary cartilage degeneration by acute synovitis.

474 In contrast to the histological OA pathologies observed at 2 weeks, there were no
475 significant differences in the synovitis and OARSI score at 6 and 10 weeks between the ACL-
476 T and ACL-R groups. This suggests that mechanical stress with joint instability has a much
477 greater impact on cartilage degeneration in the long term, rather than acute synovitis, in the
478 progression of OA.

479 This study has two limitations: first, we could not exclude the intra-patellar fat pad
480 (IFP) when synovium was collected from the knee joint. Therefore, the result of real-time
481 PCR for synovium might reflect the biological changes of IFP to synovitis and mechanical
482 stress. The second is that miRNA-derived cells were not clarified. Synovial fluid components
483 reflect biological changes of various articular tissues, not only synovium and cartilage;
484 therefore, we need to perform additional in vitro experiments to investigate the tissue
485 interaction between synovium and cartilage in detail.

486 In conclusion, we successfully established a novel method for collecting synovial
487 fluid in the murine knee joint using Tetra-slime. During the OA progression, acute synovitis
488 led to secondary cartilage degeneration in the early stage, which might be attributed to the

489 increase of MMP-3, TNF-α, and M1 macrophage activation in the synovium. Among this

490 tissue interaction, synovial fluid might play a role in preventing cartilage degeneration by

491 increasing miR145-5p and miR149-5p. Whereas in the middle and late stages, mechanical

492 stress was a more critical factor in the progression of cartilage degeneration rather than

493 synovitis (Fig. 8).

494

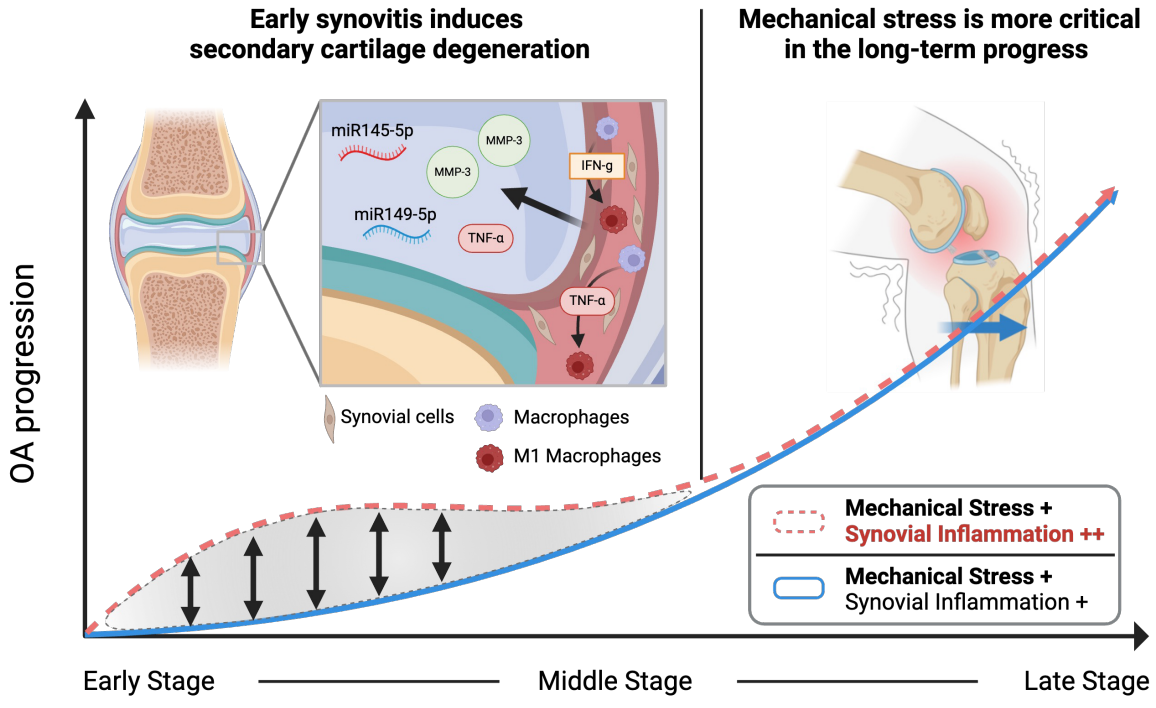

495

496 Fig. 8. Schematic mechanism of OA development with acute synovitis and chronic

497 mechanical stress. Acute synovitis caused secondary cartilage degeneration in the early stage

498 and MMP-3, TNF-α, and M1 macrophage activation in the synovium were involved in this

499 tissue interaction. Furthermore, miR145-5p and miR149-5p were secreted into the synovial

500 fluid to protect secondary cartilage deterioration during the same time. Unlike the early stage,

continuous mechanical stress had a much greater impact on cartilage degeneration rather than synovitis after the middle stage.

Acknowledgments

The author(s) received no financial support for the research, authorship, and/or publication of this article. The study design and summary scheme were created with BioRender.com.

Author contributions

All authors approved the final submitted manuscript.

Study design: KT.

Data collection: KT

Histological analysis: KT, KA, and SE.

Biological analysis: KT, TY, TK, and TS.

Manuscript composition: KT, TK.

Role of funding source

This study was supported by the Grant-in-Aid for JSPS Research Fellows (22J23384) to KT and Grant-in-Aid for JSPS Challenging Research (Exploratory)(21K19724) to TK.

Competing interest statement

All authors have no conflicts of interest related to the manuscript.

References

1. Han S. Osteoarthritis year in review 2022: biology. Osteoarthritis Cartilage 2022;30:1575–82.
2. Karsdal MA, Christiansen C, Ladel C, Henriksen K, Kraus VB, Bay–Jensen AC. Osteoarthritis——a case for personalized health care? Osteoarthritis Cartilage 2014;22:7–16.
3. Kuyinu EL, Narayanan G, Nair LS, Laurencin CT. Animal models of osteoarthritis: classification, update, and measurement of outcomes. J Orthop Surg Res 2016;11:19.
4. Peters H, Rockel JS, Little CB, Kapoor M. Synovial fluid as a complex molecular pool contributing to knee osteoarthritis. Nat Rev Rheumatol 2025;21:447–64.
5. Plsikova Matejova J, Spakova T, Harvanova D, Lacko M, Filip V, Sepitka R, *et al.* A Preliminary Study of Combined Detection of COMP, TIMP–1, and MMP–3 in Synovial Fluid: Potential Indicators of Osteoarthritis Progression. Cartilage 2021;13:1421S–30S.
6. Rajandran SN, Ma CA, Tan JR, Liu J, Wong SBS, Leung YY. Exploring the Association of Innate Immunity Biomarkers With MRI Features in Both Early and Late Stages Osteoarthritis. Front Med (Lausanne) 2020;7:554669.
7. Tavallaee G, Rockel JS, Lively S, Kapoor M. MicroRNAs in Synovial Pathology Associated With Osteoarthritis. Front Med (Lausanne) 2020;7:376.
8. Cortez MA, Bueso–Ramos C, Ferdin J, Lopez–Berestein G, Sood AK, Calin GA. MicroRNAs in body fluids——the mix of hormones and biomarkers. Nat Rev Clin Oncol 2011;8:467–77.
9. Li YH, Tavallaee G, Tokar T, Nakamura A, Sundararajan K, Weston A, *et al.* Identification of synovial fluid microRNA signature in knee osteoarthritis: differentiating early– and late–stage knee osteoarthritis. Osteoarthritis Cartilage 2016;24:1577–86.
10. Xie W, Su W, Xia H, Wang Z, Su C, Su B. Synovial Fluid MicroRNA–210 as a Potential Biomarker for Early Prediction of Osteoarthritis. Biomed Res Int 2019;2019:7165406.
11. Boffa A, Merli G, Andriolo L, Lattermann C, Salzmann GM, Filardo G. Synovial Fluid Biomarkers in Knee Osteoarthritis: A Systematic Review and Quantitative Evaluation Using BIPEDs Criteria. Cartilage 2021;13:82S–103S.
12. Sousa–Valente J, Calvo L, Vacca V, Simeoli R, Arevalo JC, Malcangio M. Role of TrkA signalling and mast cells in the initiation of osteoarthritis pain in the monoiodoacetate model. Osteoarthritis Cartilage 2018;26:84–94.

13. Keeble J, Blades M, Pitzalis C, Castro da Rocha FA, Brain SD. The role of substance P in microvascular responses in murine joint inflammation. Br J Pharmacol 2005;144:1059–66.
14. Keeble J, Russell F, Curtis B, Starr A, Pinter E, Brain SD. Involvement of transient receptor potential vanilloid 1 in the vascular and hyperalgesic components of joint inflammation. Arthritis Rheum 2005;52:3248–56.
15. Seifer DR, Furman BD, Guilak F, Olson SA, Brooks SC, 3rd, Kraus VB. Novel synovial fluid recovery method allows for quantification of a marker of arthritis in mice. Osteoarthritis Cartilage 2008;16:1532–8.
16. Hong S, Yu T, Wang Z, Lee CH. Biomaterials for reliable wearable health monitoring: Applications in skin and eye integration. Biomaterials 2025;314:122862.
17. Wang H. Biomaterials in Medical Applications. Polymers (Basel) 2023;15.
18. Trucillo P. Biomaterials for Drug Delivery and Human Applications. Materials (Basel) 2024;17.
19. Fang G, Bian Z, Liu D, Wu G, Wang H, Wu Z, *et al.* Water–soluble diboronic acid–based fluorescent sensors recognizing d–sorbitol. New Journal of Chemistry 2019;43:13802–9.
20. Katashima T, Kudo R, Naito M, Nagatoishi S, Miyata K, Chung UI, *et al.* Experimental Comparison of Bond Lifetime and Viscoelastic Relaxation in Transient Networks with Well–Controlled Structures. ACS Macro Lett 2022;11:753–9.
21. Takahata K, Arakawa K, Enomoto S, Usami Y, Nogi K, Saitou R, *et al.* Joint instability causes catabolic enzyme production in chondrocytes prior to synovial cells in novel non–invasive ACL ruptured mouse model. Osteoarthritis Cartilage 2022.
22. Arakawa K, Takahata K, Enomoto S, Oka Y, Ozone K, Nakagaki S, *et al.* The difference in joint instability affects the onset of cartilage degeneration or subchondral bone changes. Osteoarthritis Cartilage 2022;30:451–60.
23. Glasson SS, Chambers MG, Van Den Berg WB, Little CB. The OARSI histopathology initiative – recommendations for histological assessments of osteoarthritis in the mouse. Osteoarthritis Cartilage 2010;18 Suppl 3:S17–23.
24. Krenn V, Morawietz L, Burmester GR, Kinne RW, Mueller–Ladner U, Muller B, *et al.* Synovitis score: discrimination between chronic low–grade and high–grade synovitis. Histopathology 2006;49:358–64.
25. Livak KJ, Schmittgen TD. Analysis of relative gene expression data using real–time quantitative PCR and the 2(–Delta Delta C(T)) Method. Methods 2001;25:402–8.
26. Takahashi K, Goomer RS, Harwood F, Kubo T, Hirasawa Y, Amiel D. The effects of hyaluronan on matrix metalloproteinase–3 (MMP–3), interleukin–1a(IL–1a), and tissue inhibitor of metalloproteinase–1 (TIMP–1) gene expression during the development of osteoarthritis. Osteoarthritis Cartilage 1999;2:182–90.
27. Zhang H, Cai D, Bai X. Macrophages regulate the progression of osteoarthritis. Osteoarthritis Cartilage 2020;28:555–61.

590 28. Wu CL, Harasymowicz NS, Klimak MA, Collins KH, Guilak F. The role of macrophages in
591 osteoarthritis and cartilage repair. Osteoarthritis Cartilage 2020;28:544–54.
592 29. Fernandes TL, Gomoll AH, Lattermann C, Hernandez AJ, Bueno DF, Amano MT. Macrophage: A
593 Potential Target on Cartilage Regeneration. Front Immunol 2020;11:111.
594 30. Zhao K, Ruan J, Nie L, Ye X, Li J. Effects of synovial macrophages in osteoarthritis. Front Immunol
595 2023;14:1164137.
596 31. Hu G, Zhao X, Wang C, Geng Y, Zhao J, Xu J, *et al.* MicroRNA–145 attenuates TNF–alpha–driven
597 cartilage matrix degradation in osteoarthritis via direct suppression of MKK4. Cell Death Dis
598 2017;8:e3140.
599 32. Santini P, Politi L, Vedova PD, Scandurra R, Scotto dAbusco A. The inflammatory circuitry of miR–
600 149 as a pathological mechanism in osteoarthritis. Rheumatol Int 2014;34:711–6.
601 33. Chiu YS, Bamodu OA, Fong IH, Lee WH, Lin CC, Lu CH, *et al.* The JAK inhibitor Tofacitinib inhibits
602 structural damage in osteoarthritis by modulating JAK1/TNF–alpha/IL–6 signaling through Mir–
603 149–5p. Bone 2021;151:116024.
604 34. de Lange–Brokaar BJ, Ioan–Facsinay A, van Osch GJ, Zuurmond AM, Schoones J, Toes RE, *et al.*
605 Synovial inflammation, immune cells and their cytokines in osteoarthritis: a review.
606 Osteoarthritis Cartilage 2012;20:1484–99.
607 35. Nefla M, Holzinger D, Berenbaum F, Jacques C. The danger from within: alarmins in arthritis. Nat
608 Rev Rheumatol 2016;12:669–83.
609 36. Lopes EBP, Filiberti A, Husain SA, Humphrey MB. Immune Contributions to Osteoarthritis. Curr
610 Osteoporos Rep 2017;15:593–600.
611 37. Lambert C, Zappia J, Sanchez C, Florin A, Dubuc JE, Henrotin Y. The Damage–Associated Molecular
612 Patterns (DAMPs) as Potential Targets to Treat Osteoarthritis: Perspectives From a Review of the
613 Literature. Front Med (Lausanne) 2020;7:607186.
614 38. Liu–Bryan R. Synovium and the innate inflammatory network in osteoarthritis progression. Curr
615 Rheumatol Rep 2013;15:323.
616 39. Bartels YL, van Lent P, van der Kraan PM, Blom AB, Bonger KM, van den Bosch MHJ. Inhibition of
617 TLR4 signalling to dampen joint inflammation in osteoarthritis. Rheumatology (Oxford)
618 2024;63:608–18.
619 40. Pauly HM, Larson BE, Coatney GA, Button KD, DeCamp CE, Fajardo RS, *et al.* Assessment of cortical
620 and trabecular bone changes in two models of post–traumatic osteoarthritis. J Orthop Res
621 2015;33:1835–45.
622 41. Maerz T, Newton MD, Kurdziel MD, Altman P, Anderson K, Matthew HW, *et al.* Articular cartilage
623 degeneration following anterior cruciate ligament injury: a comparison of surgical transection and
624 noninvasive rupture as preclinical models of post–traumatic osteoarthritis. Osteoarthritis
625 Cartilage 2016;24:1918–27.

42. Gilbert SJ, Bonnet CS, Stadnik P, Duance VC, Mason DJ, Blain EJ. Inflammatory and degenerative phases resulting from anterior cruciate rupture in a non–invasive murine model of post–traumatic osteoarthritis. J Orthop Res 2018;36:2118–27.
43. Chen JJ, Huang JF, Du WX, Tong PJ. Expression and significance of MMP3 in synovium of knee joint at different stage in osteoarthritis patients. Asian Pac J Trop Med 2014;7:297–300.
44. Murphy G, Nagase H. Progress in matrix metalloproteinase research. Mol Aspects Med 2008;29:290–308.
45. Blom AB, van Lent PL, Libregts S, Holthuysen AE, van der Kraan PM, van Rooijen N, *et al.* Crucial role of macrophages in matrix metalloproteinase–mediated cartilage destruction during experimental osteoarthritis: involvement of matrix metalloproteinase 3. Arthritis Rheum 2007;56:147–57.
46. Bondeson J, Wainwright SD, Lauder S, Amos N, Hughes CE. The role of synovial macrophages and macrophage–produced cytokines in driving aggrecanases, matrix metalloproteinases, and other destructive and inflammatory responses in osteoarthritis. Arthritis Res Ther 2006;8:R187.
47. Munjal A, Bapat S, Hubbard D, Hunter M, Kolhe R, Fulzele S. Advances in Molecular biomarker for early diagnosis of Osteoarthritis. Biomol Concepts 2019;10:111–9.
48. Palma AD, Cheleschi S, Pascarelli NA, Tenti S, Galeazzim M, Fioravanti A. Do microRNAs have a key epigenetic role in osteoarthritis and in mechanotransduction? Clin Exp Rheumatol 2016;35 518–26.